Pericyclic Reaction of Ketenes with Cascade Reaction Products of Pyridine *N*-Oxides and Dipolarophiles. X-Ray Structures of the Adducts and Formation Mechanism

Shigeru OISO, Masashi ETO,[1)] Yasuyuki YOSHITAKE, and Kazunobu HARANO*

Graduate School of Pharmaceutical Sciences, Kumamoto University; 5–1 Oe honmachi, Kumamoto 862–0973, Japan.
Received May 28, 2003; accepted July 17, 2003; published online July 17, 2003

The structures of the adducts derived from the reactions of substituted ketenes with dihydropyridine derivatives have been clarified by single crystal X-ray analyses and the formation mechanism is discussed on the basis of the reaction-path calculations by semiempirical and density functional theory (DFT) molecular orbital methods.

Key words ketene; dihydropyridine; imine; cycloaddition; density functional theory; X-ray analysis

Previously, we reported that the reactions of pyridine *N*-oxides with phenylsulfonylallene (**2**) gave the 1,5-sigmatropic rearrangement products (**1**) of the 1 : 1 cycloadducts and the 1 : 2 azetidine-type cycloadducts (**3**) (Chart 1).[2)]

Isolated 1 : 1 adducts (**1**) reacted with **2** to give the 1 : 2 adducts (**3**). The similar reactions occurred with the dihydropyridine derivatives (**1a**—**e**) derived from the cascade reactions of pyridine *N*-oxides with phenyl isocyanates[3)] and *N*-arylmaleimides.[4)]

For the azetidine formation reaction, we have proposed a sequential pericyclic reaction pathway which consists of the [4+2] cycloaddition followed by the [3,3]-sigmatropic rearrangement of the [4+2] cycloadduct (Path A in Chart 2).

On the other hand, Machiguchi *et al.* revealed that the so-called "[2+2] adducts" of ketenes and cyclic dienes are derived from the [3,3]-sigmatropic rearrangements of the initially formed [4+2] cycloadducts (**4**) of the dienes and the ketene carbonyl groups.[5)]

However, this reaction mechanism may not be applicable to the reaction of 1-azadienes. The molecular orbital (MO) calculation of the reaction pathway suggests that the reaction proceeds *via* a stepwise [2+2] cycloadditiion that is initiated by the imine nucleophile attacking the ketene, followed by cyclization of the 2-azadiene intermediate (**5**) (Path B). Isolation of two stereoisomeric 2 : 1 cycloadducts from the reaction of 3,3-dimethyl-3*H*-indole with **2** strongly supports the presence of a zwitterionic reaction intermediate.[6)]

Although ketenes prefer to undergo [2+2] cycloadditions with imines, some azadienes have been reported to undergo [4+2] cycloadditions with diphenylketene.[7,8)]

In this paper, we wish to discuss the reaction behavior of ketenes toward the dihydropyridines such as **1a**—**f** on the basis of the X-ray structures of the adducts and MO calculation data.

Results and Discussion

The reactions were carried out between three ketenes (**6a**—**c**) and four dihydropyridine derivatives (**1a**—**d**) derived from the cascade pericyclic reactions of pyridine *N*-oxides and phenyl isocyanate.[3)] The reaction conditions and products are summarized in Chart 3 and Table 1. The structures of the adducts are determined on the basis of the spectral data of a pair of the adducts (**7aa**, **8aa**) of methoxyketene (**6a**) and **1a**, whose structures are established by X-ray crystallography.

The reaction of **1a** with **6a** at room temperature gave a mixture of **7aa** and **8aa**. The mass spectra indicated the 1 : 1 adduct [M^+ (*m*/*z* 314)] (Fig. 1). The IR spectrum of **7aa** showed the carbonyl absorption at 1772 cm^{-1}. The ^{1}H-NMR spectrum showed three methyl signals at 1.65, 1.90 and 3.45 ppm. Comparison of the spectrum with those of the structurally-related compounds indicated that the two low-field methine protons (5.59, 5.83 ppm) were assignable to the olefinic and N–C<u>H</u>–N methine protons, respectively. H–H

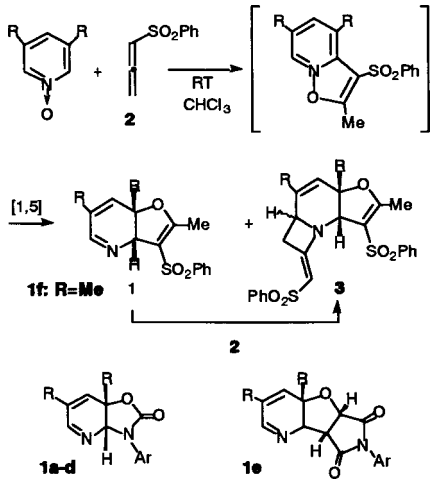

Chart 1

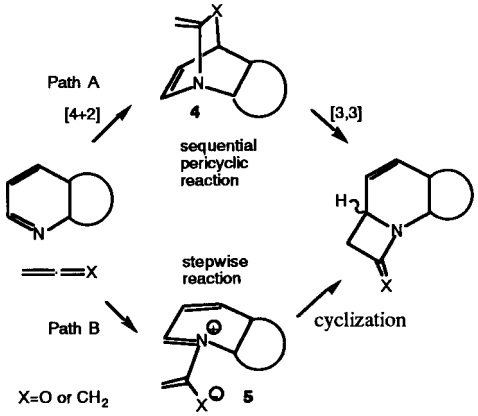

Chart 2

* To whom correspondence should be addressed. e-mail: harano@gpo.kumamoto-u.ac.jp

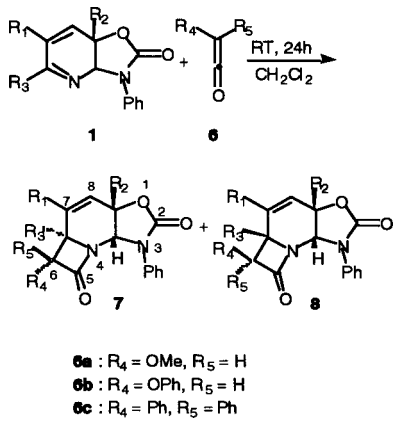

Chart 3

Table 1. Reaction of **1** with **6** at Room Temperature

1	R_1	R_2	R_3	**6**	Product (Yield % (**7**+**8**))	Ratio (**7** : **8**)
1a	Me	Me	H	**6a**	**7aa**, **8aa** (98)	1.5 : 1
1a	Me	Me	H	**6b**	**7ab** (85)	1 : 0
1a	Me	Me	H	**6c**	**7ac** (92)	1 : 0
1b	H	Me	H	**6a**	**7ba**, **8ba** (75)	2.6 : 1
1b	H	Me	H	**6b**	**7bb** (97)	1 : 0
1b	H	Me	H	**6c**	**7bc** (86)	1 : 0
1c	Me	H	Ph	**6a**	**8ca** (80)	0 : 1
1c	Me	H	Ph	**6b**	**7cb**, **8cb** (88)	1 : 1.2
1c	Me	H	Ph	**6c**	**7cc** (45)	1 : 0
1d	H	H	Ph	**6a**	**7da**, **8da** (49)	1 : 2.5
1d	H	H	Ph	**6b**	**7db**, **8db** (84)	1 : 1.3
1d	H	H	Ph	**6c**	**7dc** (75)	1 : 0

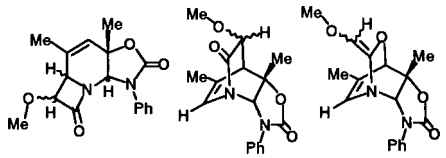

Fig. 1. Possible Reaction Products

correlation was observed between the methine protons at 3.80 and 4.27 ppm.

On the other hand, the IR spectrum of **8aa** showed two carbonyl absorption bands at 1750 and 1678 cm^{-1}. The methine proton (>N–C<u>H</u>–N<) resonates at 4.96 ppm, 0.87 ppm higher than that of **7aa**. The MS and ^{13}C-NMR spectra of both compounds resemble each other.

To know the structures of the adducts, we performed single crystal X-ray analyses of **7aa** and **8aa**. The ORTEP[9] drawings are depicted in Figs. 2a, b. As shown in Fig. 2, the adducts are not Diels–Alder adducts but azetidin-2-one ([2+2]) derivatives in which the C=N group of the dihydropyridine moieties reacted as a 2π-source. The X-ray analyses clarified that **7aa** has an *anti* relationship between the azetidin-2-one ring and oxazolone ring fused to the dihydropyridine ring whereas **8aa** has a *syn* configuration. Inspection of the dihedral angles of the four- and five-membered rings showed that the azetidin-2-one rings are almost planar whereas the oxazolone rings are distorted by the ring strain (Table 2).

The large difference (about 0.9 ppm) in the chemical shift of the N–C<u>H</u>–N proton (C4–<u>H</u> in ORTEP numbering) between **7aa** and **8aa** is attributable to the fact that the proton is located at an effective deshielding region of the amide carbonyl in **7aa**. The distance between the carbonyl group and C4–<u>H</u> is 2.91 Å for **7aa** and 4.04 Å for **8aa**.

The bond elongation[10] is found at the C7–C8 bond of the azetidin-2-one moiety in **7aa** (1.571, 1.545 Å for **7aa**, **8aa**, respectively).

As shown in Table 1, the [2+2] cycloaddition behavior was exclusively observed in the reactions of **6a**—**c** with the other dihydropyridine derivatives (**1a**—**d**) derived from the cascade reactions of pyridine, picoline and lutidine *N*-oxides with phenylisocyanate.

The phenyl substituent at the reaction site of the azadiene moiety did not interfere with the addition reaction, in sharp contrast to the reaction behavior of phenylsulfonylpropadiene.[2] Roughly speaking, the presence of a phenyl group on the imino group favors formation of the *syn* adduct whereas bulkier diphenylketene favors formation of the *anti* adduct because of the steric reason.

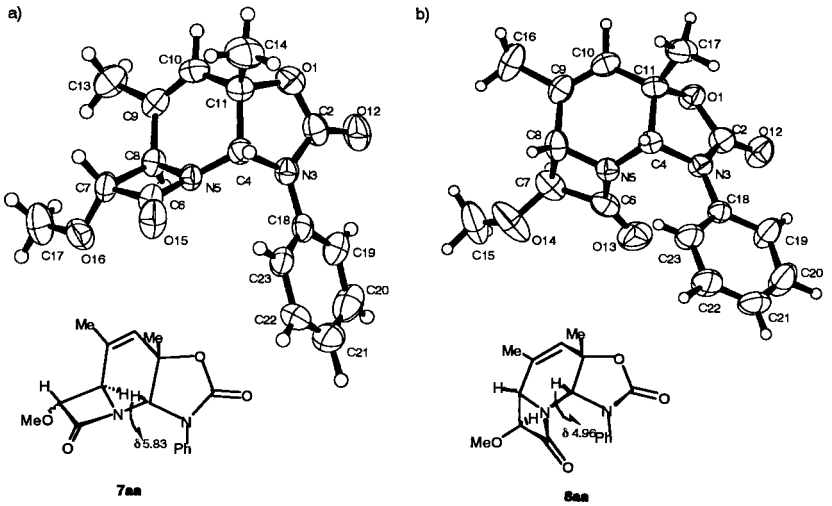

Fig. 2. ORTEP Drawings of **7aa** and **8aa**

Table 2. Important Bond Lengths, Bond Angles and Tortion Angles of **7aa** and **8aa**[a)]

Bond length (Å)					Bond angle (°)				
	5–6	6–7	7–8	5–8		5–6–7	6–7–8	7–8–5	8–5–6
7aa	1.361	1.545	1.571	1.472	**7aa**	91.4	85.6	86.4	96.6
8aa	1.374	1.517	1.541	1.452	**8aa**	91.3	86.3	86.5	95.9

Tortion angle (°)[b)]							
	5–6–7–8	6–7–8–5	1–2–3–4	2–3–4–11	3–4–11–1	4–11–1–2	11–1–2–3
7aa	0.5	0.5	3.7	6.9	7.1	5.6	1.6
8aa	1.2	1.2	9.4	24.3	28.8	25.4	11.1

a) The adduct **7aa** has two molecules per asymmetric unit. The data are calculated based on the atoms (1—23). *b*) Absolute values.

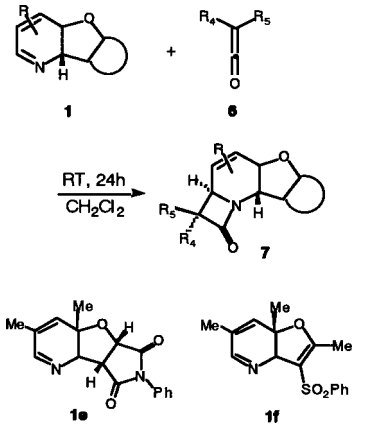

Chart 4

Table 3. Cycloaddition of **1e**, **f** with **6** at Room Temperature

1	6	Product (Yield (%))
1e	**6a**	**7ea** (49)
1e	**6b**	**7eb** (81)
1e	**6c**	**7ec** (90)
1f	**6a**	**7fa** (70)
1f	**6b**	**7fb** (83)
1f	**6c**	**7fc** (92)

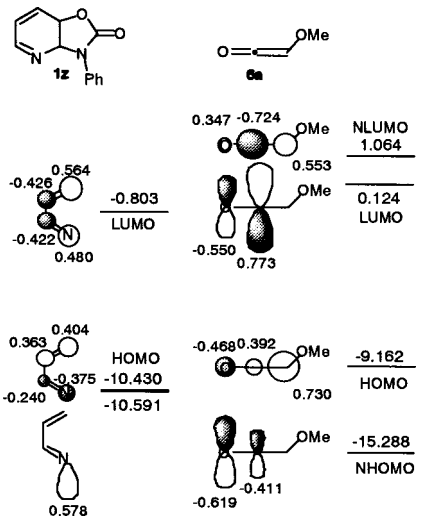

Fig. 3. FMO Orbitals of **1z** and **6a**

Next, we carried out the reactions of the ketenes with the dihydropyridine derivatives (**1e**, **f**) derived from the cascade reaction of lutidine *N*-oxide with *N*-phenylmaleimide[4)] and phenylsufonylpropadiene (Chart 4).[2)]

In the reactions with the dihydropyridines (**1e**, **f**), the [2+2] cycloadducts were also produced in good yields without formation of the *syn* isomer (Table 3). The ketenes probably attack the imino group from a less hindered site to avoid possible interaction with the residues derived from the dipolarophiles.

The frontier molecular orbital (FMO) energy levels and coefficients of the related compounds are shown in Fig. 3.[11)] From the FMO point of view,[12,13)] both [4+2] and [2+2] cycloadditions are possible. When only the FMO energy levels are considered, the interaction between the LUMO of the dihydropyridine and the HOMO of the ketene is dominant, leading to the [4+2] cycloaddition.

However, the experimental results are inconsistent with the FMO prediction. Inspection of the FMOs involving NHOMO (next HOMO) and NLUMO (next LUMO) indicates that there are very large coefficients localized at the nitrogen lone pair of the azadiene moiety and the carbonyl carbon of the ketene, indicating that the stepwise [2+2] addition is favorable (see the opposite FMO interaction).

To clarify the formation mechanism, we performed the reaction-path calculation using a simple model cycloaddition reaction of 3a,7a-dihydro-3*H*-oxazolo[4,5-*b*]pyridin-2-one with unsubstituted ketene using AM1[11)] semiempirical molecular orbital technique. The transition-state geometries and energies of the [2+2] and [4+2] cycloadditions are shown in Fig. 4.

The transition structures of the [4+2] cycloadditions were located by SADDLE and TS calculations. As pointed out in the preceding paper[6)] concerning the reaction of **1a** with allenes, the reaction of ketenes probably takes place *via* a stepwise process.

In accordance with this prediction, the reaction pathway was investigated. The transition state (**TS1**) for the >N–CO bond formation, the zwitterionic intermediate (**IM**) and the transition state (**TS2**) for the second-step ring closure could be located. The overall reaction profile is depicted in Fig. 4. The density functional theory (DFT) calculation[14)] at B3LYP/6-31G(d) level supports the AM1-calculated reaction profile.

The AM1-calculated reaction barrier for **TS2** is

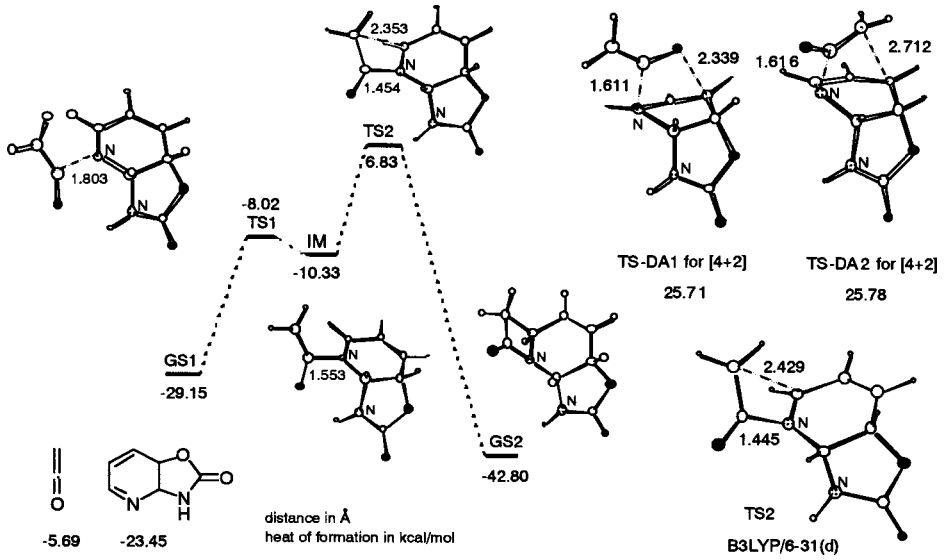

Fig. 4. Reaction Profile for Cycloaddition of the Dihydropyradine and Ketene Calculated by AM1 Method

Table 4. AM1 Heats of Formation (kcal/mol) for the *syn*/*anti* Adduct Formation and B3LYP/6-31G(d) Energies (Hartree) for the *anti* Adduct

State	AM1		B3LYP/6-31G(d)
	syn (**8**)	*anti* (**7**)	*anti* (**7**)[a,b]
GS1[c]	−29.15	−29.15	−644.77557 (0.0)
TS1	−6.26	−8.01	−644.76621 (5.87)
IM	−7.54	−10.33	−644.76761 (5.50)
TS2	6.34	6.83	−644.75063 (15.7)
GS2	−43.21	−42.80	−644.82548 (−31.4)

a) Relative energy (kcal/mol) in parentheses. *b*) TS-DA1: −644.72410 (32.0) [B3LYP/6-31G(d)//3-21G]. *c*) Summation of the reactant energies.

36.0 kcal/mol and for the DFT (B3LYP/6-31G(d)) calculation is 15.7 kcal/mol. Taking into consideration the fact that the reactions proceed at room temperature, the DFT value seems to be reasonable.

Comparison of the reaction barriers ($\Delta Hf_{TS2}-\Delta Hf_{GS1}$) for the *syn* and *anti* adduct formations is listed in Table 4.

The reaction path leading to the *syn* adduct is 0.5 kcal/mol more stable than the pathway of the *anti* adduct.

The stability of **IM** seems to be important. The AM1 calculation of the intermediates of the diphenyl derivatives (see Fig. 5) indicates that **IM** (*syn*) leading to the *syn* adduct is more stable than the **IM** (*anti*), in which the C=O···H–C type interactions[15—17] between the ketene carbonyl and the neighboring Ar–H and C–H hydrogens are operative.

The substituent of addends probably modifies the relative stability of **IM** and/or **TS** based on the simple model reaction to give the observed product ratio.

As for the azetidin-2-one formation reaction, alternate reaction pathways *via* [4+2] cycloaddition are possible (Fig. 6). Path A is a cascade-type reaction (see also Chart 2).[2,5] The barrier for Path A is 18.9 kcal/mol higher than that for the stepwise [2+2] cycloaddition and 12.5 kcal/mol higher than the barrier for the corresponding cyclohexadiene model.

In Path C, the reaction barrier for the DA reaction of the azadiene with the C=C double bond of ketene is comparable to the value for Path 1. However, this reaction pathway involves a thermally forbidden [1,3]-sigmatropic rearrangement reaction which may occur by strain release of the 1-azabicyclo[2.2.2]oct-5-en-2-one moiety. These reaction pathways satisfy the stereochemistry of the adduct. In view of the MO calculated reaction barriers of the [4+2] reactions and the reaction conditions used, we can rule out these possibilities.

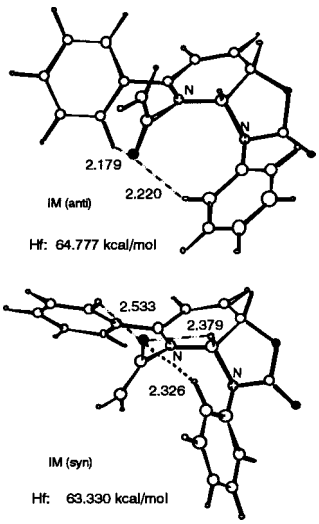

Fig. 5. >C=O···H–C Interactions in **IM**

The azadiene moiety of the 3a,7a-dihydro-3*H*-oxazolo[4,5-*b*]pyridin-2-ones did not act as the 4π-source. The reaction behavior is in contrast to the known reactions of some open-chain azadiene derivatives with ketenes.[8] The difference in the reaction behavior is probably not only due to structural features of the azadiene moieties but also due to the nature of the FMOs of both addends. Inspection of the transition structures of the [4+2] cycloadditions (Fig. 4) shows significant steric repulsions between the substituents of the addends and ring strains. On the other hand, in the stepwise [2+2] cycloaddition, the interaction between the lone pair of the nitrogen atom of **1** and the carbonyl carbon of **6** occurs from the less hindered site.

Ketenes are versatile substances for carbon skeleton con-

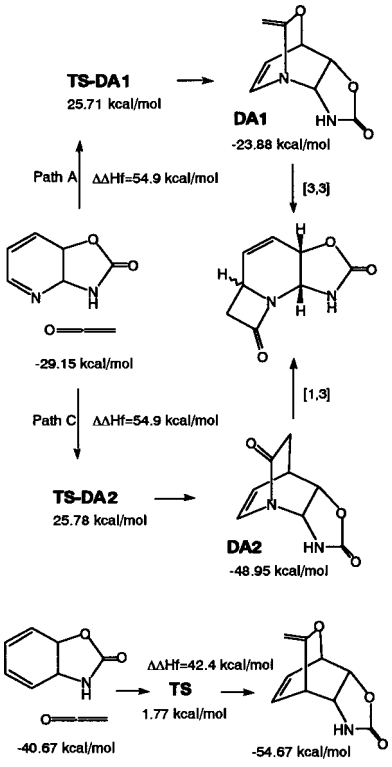

Fig. 6. Reaction Pathway *via* DA Reaction Following by Sigmatropic Rearrangement

struction because they undergo [2+2], [4+2] and [2+2+2] reactions.[18,19] In particular, the [2+2] reactions of ketenes and imines are extremely useful for preparation of β-lactams.[20]

The present reaction provides a clue for the peri and regioselective preparation method of 1-azabicyclo-[4.2.0]octan-8-one derivatives. The FMO approach and the reaction-path calculation by semiempirical MO method rationalize the reaction behavior of the ketenes toward the cyclic imines. The DFT method seems to afford much more accurate results.

Experimental

Melting points were uncorrected. The IR spectra were taken with a Hitachi 270-30 spectrophotometer. ^{1}H- and ^{13}C-NMR spectra were taken with JEOL JNM-EX 270 and JNM-A 500 spectrometers for *ca.* 10% solution ($CDCl_3$) with TMS as an internal standard. Chemical shifts are expressed as δ values and the coupling constants (J) are expressed in Hz.[21] Mass spectra were obtained using a JEOL JMS-DX 303 instrument.

Molecular Orbital Calculation Semi-empirical MO calculations were run through the ANCHOR II interface using MOPAC6.06[11] on a Fujitsu S-4/2 work station or through the CS Chem3D Pro interface using MOPAC93 on a Power Macintosh G4 computer. The NLLSQ calculations were performed on a Compaq Alpha Server ES40.

The *ab initio* and DFT calculations were carried out on a Compaq Alpha Server ES40.

The transition states (TS) were located by the transition-state location routine (SADDLE and TS).

The fully-optimized geometries calculated by AM1 or PM3 method were used as starting geometries for the *ab initio* and DFT calculations.[14] Graphical analysis of the MO calculation data was performed on a Macintosh G4 personal computer.

Material Ketenes (**6a**—**c**)[22,23] and dihydro-3*H*-oxazolo[4,5-*b*]pyridin-2-ones (**1a**—**f**)[1,3,4] were prepared according to the reported methods.

Reaction of 6a with 1a (General Method) A solution of triethylamine (0.40 g, 4 mmol) in CH_2Cl_2 (2 ml) was added to a solution of methoxyacetylchloride (0.32 g, 4 mmol) in CH_2Cl_2 (1 ml) at 0 °C. After 10 min, to this solution (crude **6a**), a solution of **1a** (1 mmol) in CH_2Cl_2 (2 ml) was added dropwise. The mixture was stirred for 24 h at room temperature. Aqueous saturated $NaCO_3$ solution was added to the reaction mixture. The organic layer was separated and the aqueous layer was extracted twice with CH_2Cl_2. The combined extract was dried over anhydrous $MgSO_4$. After evaporation of the solvent, the residue was chromatographed on silica gel to give the adducts (**7aa**, **8aa**).

7aa: Colorless prisms. mp 130—130.5 °C (from EtOH–acetone). IR (KBr) cm^{-1}: 1772 (C=O), 1596 (C=C). ^{1}H-NMR (270 MHz; $CDCl_3$) δ: 1.65 (3H, s, C8a-Me), 1.90 (3H, s, C7-Me), 3.45 (3H, br s, C6-OMe), 3.80 (1H, br s, C6a-H), 4.27 (1H, d, J=2.0, C6-H), 5.59 (1H, s, C8-H), 5.83 (1H, s, C3a-H), 7.19—7.27 (1H, m, aromatic H), 7.38—7.44 (2H, m, aromatic H), 7.58—7.61 (2H, m, aromatic H). ^{13}C-NMR (67.5 MHz; $CDCl_3$) δ: 18.6 (C7-Me), 27.1 (C8a-Me), 55.2 (C6a), 57.9 (C6-OMe), 66.4 (C3a), 73.9 (C8a), 88.6 (C6), 120.2, 124.4 (C8), 125.4, 129.3, 134.9 (N3-Ph), 135.6 (C7), 152.9 (C2), 166.5 (C5). MS (*m/z*): 314 (M^+), 270 (M^+-CO_2), 239 (M^+-CO_2-OMe). HR-MS Calcd for $C_{17}H_{18}N_2O_4$ (M^+) *m/z*: 314.1266, Found: 314.1333.

8aa: Colorless prisms. mp 105—107 °C (from EtOH–acetone). IR (KBr) cm^{-1}: 1750 (C=O), 1678 (C=O), 1600 (C=C). ^{1}H-NMR (270 MHz; $CDCl_3$) δ: 1.52 (3H, s, C8a-Me), 1.92 (3H, s, C7-Me), 3.52 (3H, br s, C6-OMe), 3.91 (1H, br s, C6a-H), 4.25 (1H, d, J=1.7, C6-H), 4.96 (1H, s, C3a-H), 5.68 (1H, s, C8-H), 7.16—7.26 (1H, m, aromatic H), 7.36—7.47 (2H, m, aromatic H), 7.64—7.67 (2H, m, aromatic H). ^{13}C-NMR (67.5 MHz; $CDCl_3$) δ: 18.8 (C7-Me), 25.2 (C8a-Me), 57.9 (C6a), 58.4 (C6-OMe), 72.1 (C3a), 76.5 (C8a), 89.4 (C6), 120.1, 123.4 (C8), 125.3, 129.4, 137.6 (N3-Ph), 137.9 (C7), 153.5 (C2), 164.5 (C5). MS *m/z*: 314 (M^+), 270 (M^+-CO_2), 239 (M^+-CO_2-OMe). HR-MS Calcd for $C_{17}H_{18}N_2O_4$ (M^+) *m/z*: 314.1266, Found: 314.1333.

7ba: Colorless prisms. mp 150—151 °C (from EtOH–acetone). IR (KBr) cm^{-1}: 1758 (C=O), 1600 (C=C). ^{1}H-NMR (270 MHz; $CDCl_3$) δ: 1.67 (3H, s, C8a-Me), 3.43 (3H, s, C6-OMe), 3.92 (1H, dd, J=1.7, 2.0, C6a-H), 4.31 (1H, d, J=2.0, C6-H), 5.89 (1H, dd, J=10.6, 1.7, C8-H), 5.89 (1H, s, C3a-H), 6.25 (1H, dd, J=10.6, 1.7, C7-H), 7.19—7.26 (1H, m, aromatic H), 7.38—7.44 (2H, m, aromatic H), 7.56—7.59 (2H, m, aromatic H). ^{13}C-NMR (125 MHz; $CDCl_3$) δ: 26.6 (C8a-Me), 52.0 (C6a), 57.6 (C6-OMe), 67.0 (C3a), 71.8 (C8a), 89.0 (C6), 120.4, 125.5 (C8), 126.8, 129.0 (C7), 129.2, 135.5 (N2-Ph), 152.7 (C2), 166.3 (C5). MS (*m/z*): 300 (M^+), 256 (M^+-CO_2). *Anal.* Calcd for $C_{16}H_{16}N_2O_4$: C, 63.98; H, 5.38; N, 9.33: Found: C, 64.03; H, 5.14; N, 9.23%.

8ba: Colorless prisms. mp 115—116 °C (from EtOH–acetone). IR (KBr) cm^{-1}: 1756 (C=O), 1600 (C=C). ^{1}H-NMR (270 MHz; $CDCl_3$) δ: 1.53 (3H, s, C8a-Me), 3.50 (3H, s, C6-OMe), 4.04 (1H, m, C6a-H), 4.27 (1H, d, J=1.7, C6-H), 5.02 (1H, s, C3a-H), 5.98 (1H, d, J=10.6, C8-H), 6.30 (1H, dd, J=10.6, 1.7, C7-H), 7.16—7.26 (1H, m, aromatic H), 7.37—7.43 (2H, m, aromatic H), 7.64—7.67 (2H, m, aromatic H). ^{13}C-NMR (100 MHz; $CDCl_3$) δ: 24.8 (C8a-Me), 54.5 (C6a), 58.0 (C6-OMe), 72.2 (C3a), 74.3 (C8a), 89.3 (C6), 119.9, 125.1 (C8), 127.6, 128.9 (C7), 129.1, 137.5 (N2-Ph), 153.0 (C2), 164.0 (C5). MS (*m/z*): 300 (M^+), 256 (M^+-CO_2). *Anal.* Calcd for $C_{16}H_{16}N_2O_4$: C, 63.98; H, 5.38; N, 9.33: Found: C, 64.13; H, 5.26; N, 9.28%.

8ca: Colorless prisms. mp 205—206 °C (from acetone–hexane). IR (KBr) cm^{-1}: 1776 (C=O), 1600 (C=C). ^{1}H-NMR (270 MHz; $CDCl_3$) δ: 2.13 (3H, s, C7-Me), 3.26 (3H, s, C6-OMe), 4.53 (1H, s, C6-H), 4.82 (1H, dd, J=4.6, 4.3, C8a-H), 5.21 (1H, d, J=4.3, C3a-H), 6.01 (1H, dd, J=4.6, 1.3, C8-H), 7.14—7.25 (2H, m, aromatic H), 7.34—7.49 (6H, m, aromatic H), 7.52—7.62 (2H, m, aromatic H). ^{13}C-NMR (100 MHz; $CDCl_3$) δ: 19.9 (C7-Me), 58.1 (C6-OMe), 66.0 (C3a), 68.8 (C8a), 91.1 (C6), 119.2, 119.8, 124.5 (C8), 127.8, 128.1, 128.2, 128.6, 134.2 (C7), 136.7 (N2-Ph), 142.2 (C6a), 153.1 (C2), 163.8 (C5). MS (*m/z*): 376 (M^+), 331 (M^+-CO_2). *Anal.* Calcd for $C_{22}H_{20}N_2O_4$: C, 70.19; H, 5.37; N, 7.44. Found: C, 70.33; H, 5.27; N, 7.62%.

7da: Colorless prisms. mp 215—218 °C. IR (KBr) cm^{-1}: 1776, 1740 (C=O), 1598 (C=C). ^{1}H-NMR (400 MHz; $CDCl_3$) δ: 3.10 (3H, s, C6-OMe), 4.48 (1H, s, C6-H), 5.14 (1H, dd, J=8.8, 4.4, C8a-H), 6.19 (1H, dd, J=10.3, 4.4, C8-H), 6.40 (1H, d, J=8.8, C3a-H), 6.98—7.48 (11H, m, aromatic H). ^{13}C-NMR (67.5MHz; $CDCl_3$) δ: 58.6 (C6-OMe), 61.6 (C3a), 63.4 (C8a), 63.5 (C6a), 92.4 (C6), 119.8, 122.9, 125.3, 126.8, 128.3, 129.2, 134.8, 134.9, 135.4, 166.9. MS (*m/z*): 362 (M^+), 330 (M^+-OMe).

8da: Colorless prisms. mp 190—191 °C (from EtOH–acetone). IR (KBr) cm^{-1}: 1740 (C=O), 1600 (C=C). ^{1}H-NMR (270 MHz; $CDCl_3$) δ: 3.15 (3H, s, C6-OMe), 4.45 (1H, s, C6-H), 4.77 (1H, ddd, J=5.0, 5.0, 1.0, C8a-H), 5.28 (1H, d, J=5.0, C3a-H), 6.23 (1H, dd, J=10.6, 5.0, C8-H), 6.98 (1H, dd, J=10.6, 1.0, C7-H), 7.19—7.25 (1H, m, aromatic H), 7.36—7.50 (7H, m, aromatic H), 7.69—7.73 (2H, m, aromatic H). ^{13}C-NMR (67.5 MHz; $CDCl_3$)

δ: 58.6 (C6-OMe), 64.4 (C6a), 66.8 (C3a), 67.5 (C8a), 92.6 (C6), 119.9, 121.7, 125.3, 126.9, 128.6, 128.9, 129.2, 134.9, 135.0, 137.1, 153.6, 165.0. MS (*m/z*): 362 (M^+), 330 (M^+-OMe). *Anal.* Calcd for $C_{21}H_{18}N_2O_4$: C, 69.60; H, 5.01; N, 7.73. Found: C, 69.37; H, 4.99; N, 7.80%.

7ea: Colorless prisms. mp 231—232 °C (from EtOH–acetone). IR (KBr) cm^{-1}: 1768 (C=O), 1712 (C=O). ^{1}H-NMR (270 MHz; $CDCl_3$) δ: 1.40 (3H, s, C9a-Me), 1.75 (3H, s, C8-Me), 3.46 (3H, s, C7-OMe), 3.72 (1H, dd, *J*=10.9, 8.2, C4a-H), 3.79 (1H, m, C7a-H), 4.22 (1H, d, *J*=2.3, C7-H), 4.68 (1H, d, *J*=10.9, C1a-H), 4.94 (1H, d, *J*=8.2, C5a-H), 5.58 (1H, m, C9-H), 7.20—7.26 (2H, aromatic H), 7.41—7.51 (3H, aromatic H). ^{13}C-NMR (125 MHz; $CDCl_3$) δ: 19.3 (C8-Me), 27.2 (C9a-Me), 44.7 (C4a), 56.8 (C7a), 57.0 (C1a), 57.1 (C7-OMe), 76.8 (C5a), 79.1 (C9a), 89.5 (C7), 125.7, 128.6, 128.9, 129.3, 131.3, 134.3, 167.7, 171.9, 174.2. MS (*m/z*): 368 (M^+), 353 (M^+-Me), 297 ($M^+-MeO-C=C=O$). *Anal.* Calcd for $C_{20}H_{20}N_2O_5$: C, 65.21; H, 5.47; N, 7.60. Found: C, 64.80; H, 5.17; N, 7.60%.

7fa: Colorless prisms. mp 176—177 °C (from EtOH). IR (KBr) cm^{-1}: 1764 (C=O), 1624 (C=C). ^{1}H-NMR (400 MHz; $CDCl_3$) δ: 1.45 (3H, s, C8a-Me), 1.76 (3H, d, *J*=1.5, C7-Me), 2.28 (3H, d, *J*=1.5, C2-Me), 3.26 (1H, m, C6a-H), 3.44 (3H, s, C6-OMe), 4.12 (1H, m, C6-Me), 5.02 (1H, m, C3a-H), 5.32 (1H, m, C8-H), 7.52—7.63 (3H, aromatic H), 7.90—7.94 (2H, aromatic H). ^{13}C-NMR (100 MHz; $CDCl_3$) δ: 14.4 (C7-Me), 18.7 (C8a-Me), 54.4 (C6a), 57.0 (C6-OMe), 58.1 (C3a), 82.5 (C8a), 88.3 (C6), 106.9, 124.4, 127.3, 129.2, 133.0, 136.0, 141.7, 165.8, 167.6. MS (*m/z*): 376 (M^+), 234 (M^+-SO_2Ph). *Anal.* Calcd for $C_{19}H_{21}NO_5S$: C, 60.78; H, 5.64; N, 3.73. Found: C, 60.32; H, 5.48; N, 3.76%.

Reaction of 6b with 1a—c The reactions were performed according to the general method using pheoxyacethylchloride.

7ab: Colorless prisms. mp 155—158 °C. IR (KBr) cm^{-1}: 1746 (C=O), 1598 (C=C). ^{1}H-NMR (270 MHz; $CDCl_3$) δ: 1.69 (3H, s, C8a-Me), 1.87 (3H, m, C7-Me), 4.05 (1H, m, C6a-H), 4.93 (1H, d, *J*=2.3, C6-H), 5.62 (1H, dd, *J*=1.3, 1.7, C8-H), 5.88 (1H, s, C3a-H), 7.01—7.09 (3H, m, aromatic H), 7.19—7.39 (3H, m, aromatic H), 7.41—7.45 (2H, m, aromatic H), 7.58—7.69 (2H, m, aromatic H). ^{13}C-NMR (67.5 MHz; $CDCl_3$) δ: 18.5 (C7-Me), 27.1 (C8a-Me), 55.6 (C6a), 66.6 (C3a), 73.8 (C8a), 85.3 (C6), 114.6, 116.4, 120.3, 122.2, 123.1, 123.4, 124.6 (C8), 125.5, 129.1, 129.3, 129.6, 129.8, 134.8 (C6-OPh), 135.6 (N3-Ph), 152.8 (C7), 156.8 (C2), 165.9 (C5). MS (*m/z*): 376 (M^+), 333 (M^+-CO), 239 ($M^+-CO-OPh$). HR-MS Calcd for $C_{22}H_{20}N_2O_4$ (M^+) *m/z*: 376.1423, Found: 376.1411.

7bb: Colorless prisms. mp 178—180 °C (from EtOH–acetone). IR (KBr) cm^{-1}: 1766 (C=O), 1598 (C=C). ^{1}H-NMR (270 MHz; $CDCl_3$) δ: 1.73 (3H, s, C8a-Me), 4.10 (1H, dd, *J*=2.0, 1.3, C6a-H), 4.94 (1H, d, *J*=2.0, C6-H), 6.00 (2H, m, C3a-H, C8-H), 6.37 (1H, dd, *J*=11.2, 1.3, C7-H), 6.94—7.07 (3H, m, aromatic H), 7.20—7.44 (5H, m, aromatic H), 7.57—7.60 (2H, m, aromatic H). ^{13}C-NMR (67.5 MHz; $CDCl_3$) δ: 26.7 (C8a-Me), 52.9 (C6a), 67.1 (C3a), 71.9 (C8a), 85.2 (C6), 115.4, 120.4, 122.9, 125.7, 126.1, 129.4, 129.7, 129.8, 135.4, 152.6, 156.6, 165.2. MS (*m/z*): 362 (M^+), 318 (M^+-CO_2). *Anal.* Calcd for $C_{21}H_{18}N_2O_4$: C, 69.60; H, 5.01; N, 7.73. Found: C, 69.54; H, 4.99; N, 7.76%.

7cb: Colorless prisms. mp 165—166 °C (from EtOH–acetone). IR (KBr) cm^{-1}: 1778 (C=O), 1740 (C=O), 1598 (C=C). ^{1}H-NMR (270 MHz; $CDCl_3$) δ: 2.18 (3H, t, *J*=1.3, C7-Me), 5.30 (1H, dd, *J*=8.6, 5.3, C8a-H), 5.36 (1H, s, C6-H), 6.13 (1H, dd, *J*=5.3, 1.3, C8-H), 6.33 (1H, d, *J*=8.6, C3a-H), 6.98—7.46 (15H, aromatic H). ^{13}C-NMR (67.5 MHz; $CDCl_3$) δ: 19.9 (C7-Me), 61.2 (C3a), 65.3 (C8a), 65.7 (C6a), 87.3 (C6), 116.5, 119.4, 120.7, 122.8, 124.6, 127.7, 127.9, 128.1, 128.5, 129.2, 133.6, 134.7, 143.3, 152.5, 156.6, 165.3. MS (*m/z*): 438 (M^+), 345 (M^+-OPh), 301 ($M^+-OPh-CO_2$), 259 ($M^+-OPh-CO_2-C_2H_2O$). *Anal.* Calcd for $C_{27}H_{22}N_2O_4$: C, 73.96; H, 5.06; N, 6.39. Found: C, 73.60; H, 4.94; N, 6.40%.

8cb: Colorless prisms. mp 181—183 °C. IR (KBr) cm^{-1}: 1776 (C=O), 1596 (C=C). ^{1}H-NMR (270 MHz; $CDCl_3$) δ: 2.09 (3H, t, *J*=1.3, C7-Me), 4.87 (1H, dd, *J*=5.3, 4.6, C8a-H), 5.23 (1H, s, C6-H), 5.38 (1H, d, *J*=5.3, C3a-H), 6.02 (1H, dd, *J*=4.6, 1.3, C8-H), 6.80—7.68 (15H, aromatic H). ^{13}C-NMR (67.5 MHz; $CDCl_3$) δ: 20.4 (C7-Me), 66.7 (C3a), 67.2 (C6a), 69.1 (C8a), 87.8 (C6), 116.7, 119.6, 120.1, 122.9, 125.1, 128.3, 128.4, 128.5, 128.8, 129.2, 129.6, 134.6, 137.2, 142.6, 153.5, 157.2,164.2. MS (*m/z*): 438 (M^+), 345 (M^+-OPh), 301 ($M^+-OPh-CO_2$). *Anal.* Calcd for $C_{27}H_{22}N_2O_4$: C, 73.96; H, 5.06; N, 6.39. Found: C, 73.67; H, 5.02; N, 6.37%.

7db: Colorless prisms. mp 167—169 °C (from benzene). IR (KBr) cm^{-1}: 1782 (C=O), 1748 (C=O), 1598 (C=C). ^{1}H-NMR (270 MHz; $CDCl_3$) δ: 5.20 (1H, dd, *J*=8.3, 4.6, C8a-H), 5.21 (1H, s, C6-H), 6.27 (1H, dd, *J*=10.6, 4.6, C8-H), 6.49 (1H, d, *J*=8.3, C3a-H), 6.65—6.69 (2H, m, C7-H and aromatic H), 6.89—7.51 (14H, m, aromatic H). ^{13}C-NMR (67.5 MHz; $CDCl_3$) δ: 61.7 (C3a), 63.5 (C8a), 77.2 (C6a), 88.3 (C6), 115.7, 119.9, 122.7, 123.5, 125.3, 126.9, 128.1, 128.3, 129.3, 129.5, 134.1, 134.4, 135.4, 144.8, 156.5, 165.9. MS (*m/z*): 424 (M^+), 330 (M^+-OPh). *Anal.* Calcd for $C_{21}H_{18}N_2O_4$: C, 73.57; H, 4.75; N, 6.60. Found: C, 73.62; H, 4.62; N, 6.61%.

8db: Colorless prisms. mp 242—244 °C (from EtOH–acetone) IR (KBr) cm^{-1}: 1774 (C=O), 1598 (C=C). ^{1}H-NMR (270 MHz; $CDCl_3$) δ: 4.83 (1H, td, *J*=4.6, 1.3, C8a-H), 5.19 (1H, s, C6-H), 5.37 (1H, d, *J*=4.6, C3a-H), 6.31 (1H, dd, *J*=10.6, 4.6, C8-H), 6.69—6.74 (2H, m, aromatic H), 6.88—6.93 (1H, m, aromatic H), 7.05—7.49 (11H, m, aromatic H and C7-H), 7.72—7.77 (2H, m, aromatic H). ^{13}C-NMR (67.5 MHz; $CDCl_3$) δ: 64.6 (C6a), 66.9 (C3a), 67.5 (C8a), 88.5 (C6), 115.8, 119.9, 122.3, 122.6, 125.4, 127.0, 128.7, 129.3, 129.4, 134.4, 137.0, 153.5, 156.7, 164.0. MS (*m/z*): 424 (M^+), 330 (M^+-OPh). *Anal.* Calcd for $C_{21}H_{18}N_2O_4$: C, 73.57; H, 4.75; N, 6.60. Found: C, 73.30; H, 4.76; N, 6.49%.

7eb: Colorless prisms. mp 265—270 °C (from EtOH–acetone). IR (KBr) cm^{-1}: 1768, 1710 (C=O). ^{1}H-NMR (400 MHz; $CDCl_3$) δ: 1.45 (3H, s, C9a-Me), 1.74 (3H, s, C8-Me), 3.76 (1H, dd, *J*=10.6, 8.1, C4a-H), 4.02 (1H, m, C7a-H), 4.74 (1H, d, *J*=10.6, C1a-H), 4.82 (1H, d, *J*=2.2, C7-H), 4.96 (1H, d, *J*=8.1, C5a-H), 5.62 (1H, m, C9-H), 7.02—7.08 (3H, aromatic H), 7.23—7.50 (7H, aromatic H). ^{13}C-NMR (125 MHz; $CDCl_3$) δ: 19.4 (C8-Me), 27.1 (C9a-Me), 44.7 (C4a), 57.3 (C7a), 57.7 (C1a), 76.7 (C5a), 79.1 (C9a), 85.9 (C7), 116.2, 122.8, 125.6, 129.0, 129.3, 129.7, 131.2 (4), 133.9 (4), 157.0 (4), 167.1 (4), 171.9 (4), 174.2 (4). MS (*m/z*): 430 (M^+), 297 ($M^+-PhO-C=C=O$). *Anal.* Calcd. for $C_{25}H_{22}N_2O_5$: C, 69.76; H, 5.15; N, 6.51. Found: C, 69.99; H, 5.08; N, 6.65%.

7fb: Colorless prisms. mp 182—183 °C (from EtOH). IR (KBr) cm^{-1}: 1772 (C=O), 1632 (C=C), 1596 (C=C), 1304, 1138 (–SO_2–). ^{1}H-NMR (270 MHz; $CDCl_3$) δ: 1.49 (3H, s, C8a), 1.71 (3H, s, C7-Me), 2.29 (3H, d, *J*=1.3, C2-Me), 3.20 (1H, m, C6a-H), 4.70 (1H, d, *J*=2.0, C6-H), 5.15 (1H, m, C3a-H), 5.35 (1H, m, C8-H), 7.02—7.09 (3H, aromatic H), 7.26—7.34 (2H, aromatic H), 7.49—7.63 (3H, aromatic H), 7.91—7.94 (2H, aromatic H). ^{13}C-NMR (67.5MHz; $CDCl_3$) δ: 14.3 (C8a), 18.7 (C7), 26.9 (C2), 55.3 (C6a), 58.3 (C3a), 82.2 (C8a), 84.8 (C6), 106.9, 116.2, 122.7, 124.9, 127.4, 129.2, 129.7, 133.1, 135.5, 141.7, 157.1, 164.9, 167.5. MS (*m/z*): 438 (M^+), 344 (M^+-OPh), 296 (M^+-SO_2Ph). *Anal.* Calcd for $C_{24}H_{23}NO_5S$: C, 65.89; H, 5.30; N, 3.20. Found: C, 65.62; H, 5.25; N, 3.36%.

Reaction of 6c with 1a—c The reactions were performed according to the general method uusing diphenylacetylchloride. Recrystallization from EtOH–acetone.

7ac: Colorless prisms. mp 218—219 °C. IR (KBr) cm^{-1}: 1758 (C=O). ^{1}H-NMR (270 MHz; $CDCl_3$) δ: 1.32 (3H, s, C8a-Me), 1.80 (3H, s, C7-Me), 4.52 (1H, m, C6a-H), 5.55 (1H, m, C8-H), 6.06 (1H, s, C3a-H), 7.09—7.61 (15H, m, aromatic H). ^{13}C-NMR (67.5 MHz; $CDCl_3$) δ: 18.9 (C7-Me), 26.8 (C8a-Me), 59.2 (C6a), 66.1 (C3a), 71.9 (C8a), 74.2 (C6), 120.0, 125.3, 125.6, 127.7, 127.9, 128.0, 128.1, 128.2, 128.8, 129.2, 134.9, 135.7, 136.2, 137.8, 152.9, 171.2. MS (*m/z*): 436 (M^+). *Anal.* Calcd for $C_{28}H_{24}N_2O_3$: C, 77.04; H, 5.54; N, 6.42. Found: C, 76.75; H, 5.44; N, 6.38%.

7bc: Colorless prisms. mp 198—199 °C. IR (KBr) cm^{-1}: 1738 (C=O), 1598 (C=C). ^{1}H-NMR (270 MHz; $CDCl_3$) δ: 1.63 (3H, s, C8a-Me), 4.56 (1H, dd, *J*=2.0, 1.7, C6a-H), 5.68 (1H, dd, *J*=10.9, 2.0, C7-H), 5.86 (1H, dd, *J*=10.9, 1.7, C8-H), 6.03 (1H, s, C3a-H), 7.15—7.40 (13H, m, aromatic H), 7.59—7.62 (2H, m, aromatic H). ^{13}C-NMR (67.5 MHz; $CDCl_3$) δ: 26.8 (C8a-Me), 56.1 (C6a), 67.5 (C3a), 72.4 (C8a), 73.1 (C6), 120.8, 125.9, 127.2, 127.8, 128.1, 128.2, 128.4, 128.8, 129.1, 129.2, 129.7, 135.9, 136.1, 138.9, 153.2, 171.2. MS (*m/z*): 422 (M^+).

7cc: Colorless prisms. mp 217—219 °C. IR (KBr) cm^{-1}: 3056, 1754 (C=O), 1598 (C=C). ^{1}H-NMR (270 MHz; $CDCl_3$) δ: 1.47 (3H, s, C7-Me), 5.30 (1H, dd, *J*=8.6, 5.3, C8a-H), 5.98 (1H, d, *J*=5.3, C8-H), 6.51 (1H, d, *J*=8.6, C3a-H), 6.62—6.80 (4H, m, aromatic H), 6.97—7.43 (16H, m, aromatic H). ^{13}C-NMR (67.5 MHz; $CDCl_3$) δ: 21.6 (C7-Me), 60.3 (C3a), 66.1 (8a), 70.0 (C6a), 78.5 (C6), 119.2, 122.4, 124.6, 126.9, 127.3, 127.9, 128.0, 128.1, 128.3, 128.9, 129.0, 129.4, 135.2, 135.5, 137.5, 137.9, 144.6, 152.8, 170.4. MS (*m/z*): 498 (M^+). *Anal.* Calcd for $C_{33}H_{26}N_2O_4$: C, 79.50; H, 5.26; N, 5.62. Found: C, 79.69; H, 5.38; N, 5.79%.

7dc: Colorless prisms. mp 231—233 °C. IR (KBr) cm^{-1}: 1744 (C=O), 1598 (C=C). ^{1}H-NMR (270 MHz; $CDCl_3$) δ: 5.08 (1H, dd, *J*=8.6, 5.0, C8a-H), 5.91 (1H, dd, *J*=10.9, 5.0, C8-H), 6.57 (1H, d, *J*=8.6, C3a-H), 6.76—7.76 (21H, m, C7-H and aromatic H). ^{13}C-NMR (67.5 MHz; $CDCl_3$) δ: 61.5 (C3a), 63.9 (C8a), 67.0 (C6), 78.2 (C6a), 118.9, 121.2, 124.9, 126.5, 126.9, 127.6, 127.8, 127.9, 127.9, 128.1, 128.7, 129.3, 136.0, 136.2, 136.7, 137.0, 137.6, 152.9, 172.2. MS (*m/z*): 484 (M^+). *Anal.* Calcd for $C_{32}H_{24}N_2O_3$: 79.32; H, 4.99; N, 5.78. Found: C, 79.26; H, 4.86; N, 5.86%.

7ec: Colorless prisms. mp 264—266 °C. IR (KBr) cm^{-1}: 1760, 1722 (C=O), 1596 (C=C). ^{1}H-NMR (270 MHz; $CDCl_3$) δ: 1.32 (3H, s, C9a-Me), 1.55 (3H, s, C8-Me), 3.69 (1H, dd, *J*=10.9, 8.3, C4a-H), 4.53 (1H, s, C7a-H), 4.86 (2H, m, C1a, C5a-H), 5.48 (1H, s, C9-H), 7.11—7.49 (15H, m, aro-

matic H). ^{13}C-NMR (67.5 MHz; $CDCl_3$) δ: 19.9 (C8-Me), 26.4 (C9a-Me), 45.0 (C4a), 56.8 (C7a), 60.9 (C1a), 72.5 (C7), 76.7 (C5a), 79.7 (C9a), 125.7, 127.3, 127.6, 127.8, 128.1, 128.3, 128.5, 128.8, 129.3, 130.1, 131.3, 134.5, 135.9, 138.9, 171.9, 172.3, 174.4. MS (*m*/*z*): 490 (M^+). *Anal.* Calcd for $C_{31}H_{26}N_2O_4$: C, 75.90; H, 5.34; N, 5.71. Found: C, 75.97; H, 5.22; N, 5.82%.

7fc: Colorless prisms. mp 249—251 °C. IR (KBr) cm^{-1}: 1760 (C=O), 1628 (C=C), 1318, 1160 (SO_2). ^{1}H-NMR (270 MHz; $CDCl_3$) δ: 1.10 (3H, s, C8a-Me), 1.66 (3H, s, C7-Me), 2.27 (3H, s, C2-Me), 3.54 (1H, s, C6a-H), 5.30 (1H, m, C3a-H), 5.48 (1H, m, C8-H), 6.83—7.49 (13H, m, aromatic H), 7.63—7.66 (2H, m, aromatic H). ^{13}C-NMR (67.5 MHz; $CDCl_3$) δ: 14.4 (C7-Me), 18.9 (C8a-Me), 26.7 (C2-Me), 58.1 (C6a), 59.0 (C3a), 71.0 (C8a), 82.6 (C6), 106.8, 125.6, 126.6, 127.6, 127.9, 128.1, 128.2, 128.6, 128.7, 132.5, 135.6, 136.5, 138.2, 141.6, 167.4, 170.2. MS (*m*/*z*): 496 (M^+). *Anal.* Calcd for $C_{30}H_{27}NO_4$: C, 72.41; H, 5.47; N, 2.81. Found: C, 72.37; H, 5.43; N, 2.96%.

Single Crystal X-Ray Analysis The crystal structure of **7aa** was determined as follows. The reflection data were measured on a RIGAKU AFC7R four-circle autodiffractometer with a graphite monochromated Mo-$K\alpha$ radiation (λ=0.7107 Å) and a rotating anode generator. The structure was solved by direct method. The hydrogen atoms were placed in calculated positions. The non-hydrogen atoms were refined anisotropically and the hydrogen atoms were refined isotropically. The final residuals for reflections with $I_o > 2.00\sigma I$ were R=0.086 and R_w=0.087.

Similarly, the X-ray analysis of **8aa** was performed. All calculations were performed on a Silicon Graphics O2 WS with the *teXsan*[24] Crystal Structure Analysis Package.

Crystal Data of **7aa**: $C_{17}H_{18}N_2O_4$. M=314.3, orthorhombic, a=15.422 (1), b=21.679 (3), c=9.768 (4) Å, V=3265 (1) Å^3, space group $P2_12_12_1$, Z=8, Dc=1.279, Dm=1.287 (g/cm^3). Recryst. solvent EtOH–acetone. Number of reflections collected 4218. Used for refinement 2210 ($I_o > 2.00\sigma I$). R=0.086. R_w=0.087.

Crystal Data of **8aa**: $C_{17}H_{18}N_2O_4$. M=314.3, monoclinic, a=9.663 (1), b=14.484 (2), c=11.550 (1) Å, β=97.059 (7). V=1597.4 (3) Å^3, space group $P2_1/a$, Z=4, Dc=1.307, Dm=1.296 (g/cm^3). Recryst. solvent EtOH–acetone. Number of reflections collected 3824. Used for refinement 1386 ($I_O > 3.00\sigma I$). R=0.065. R_w=0.112.

Supporting Information Available X-Ray crystallographic data for the structures (**7aa**, **8aa**) have been deposited at the Cambridge Crystallographic Data Center. The atomic coordinates of the MO-optimized structures are available from our web page (URL http://yakko.pharm.kumamoto-u.ac.jp/).

Acknowledgements We thank Professor T. Matsuoka for the useful discussion.

References and Notes

1) Present address: *School of Agriculture, Kyushu Tokai University, 5435 Kawayo, Choyoson, Asogun, Kumamoto 869–1404, Japan*.
2) Matsuoka T., Hasegawa T., Eto M., Harano K., Hisano T., *J. Chem. Soc., Perkin Trans. 2*, **1993**, 1859—1865 (1993).
3) Matsuoka T., Shinada M., Suematsu F., Harano K., Hisano T., *Chem. Pharm. Bull.*, **32**, 2077—2090 (1984).
4) Hisano T., Harano K., Matsuoka T., Yamada H., Kurihara M., *Chem. Pharm. Bull.*, **35**, 1049—1057 (1987).
5) Machiguchi T., Hasegawa T., Ishiwata A., Terashima S., Yamabe S., Minato T., *J. Am. Chem. Soc.*, **121**, 4771—4786 (1999).
6) Matsuoka T., Oiso S., Eto M., Harano K., *Tetrahedron Lett.*, **36**, 8031—8034 (1995).
7) Kollenz G., Penn G., Ott W., Peters K., Peters E.-M., Schnering H. G. von, *Heterocycles*, **26**, 625—636 (1987).
8) Buonora P., Olsen J.-C., Oh T., *Tetrahedron*, **57**, 6099—6138 (2001).
9) Johnson C. K., "ORTEP ORNL-3794," Oak Ridge National Laboratory, Tennessee, U.S.A., 1965.
10) The calculated C7–C8 bond length of **7cc** is 1.634 Å for AM1, 1.624 Å for PM3, 1.643 Å for HF/3-21G and 1.667 Å for B3LYP/6-31G(d). The ^{13}C-NMR data support this assumption. However, a single crystal suitable for the X-ray analysis has not yet been obtained.
11) AM1 calculations were performed using MOPAC 2000 ver.1.11, Fujitsu Ltd., Tokyo, Japan, 1999.
12) Fukui K., "Kagaku Hanno to Densi no Kido (Chemical Reactions and Electron Orbitals)," Maruzen, Tokyo, 1976.
13) Fleming I., "Frontier Orbitals and Organic Chemical Reactions," Wiley, London, 1976.
14) Gaussian 98, Revision A.6. Frisch M. J., Trucks G. W., Schlegel H. B., Scuseria G. E., Robb M. A., Cheeseman J. R., Zakrzewski V. G., Montgomery J. A., Jr., Stratmann R. E., Burant J. C., Dapprich S., Millam J. M., Daniels A. D., Kudin K. N., Strain M. C., Farkas O., Tomasi J., Barone V., Cossi M., Cammi R., Mennucci B., Pomelli C., Adamo C., Clifford S., Ochterski J., Petersson G. A., Ayala P. Y., Cui Q., Morokuma K., Malick D. K., Rabuck A. D., Raghavachari K., Foresman J. B., Cioslowski J., Ortiz J. V., Stefanov B. B., Liu G., Liashenko A., Piskorz P., Komaromi I., Gomperts R., Martin R. L., Fox D. J., Keith T., Al-Laham M. A., Peng C. Y., Nanayakkara A., Gonzalez C., Challacombe M., Gill P. M. W., Johnson B., Chen W., Wong M. W., Andres J. L., Gonzalez C., Head-Gordon M., Replogle E. S., Pople J. A., Gaussian, Inc., Pittsburgh PA, 1998.
15) Taylor R., Kennard O., *J. Am. Chem. Soc.*, **104**, 5063—5070 (1982).
16) Desiraju G. R., *Acc. Chem. Res.*, **24**, 290—296 (1991).
17) Steiner T., Kanters J. A., Kroon J., *Chem. Commun.*, **1996**, 1277—1278 (1996).
18) Ghosez L., O'Donnell M. J., "Pericyclic Reaction, Vol. II," Academic Press, New York, 1977, pp. 79—140.
19) Patai S., "The Chemistry of Ketenes, Allenes and Related Compounds," John Wiley & Sons Inc., New York, 1980.
20) Taggi A. E., Hafez A. M., Wack H., Young B., Ferraris D., Lectka T., *J. Am. Chem. Soc.*, **124**, 6626—6635 (2002) and references cited therein.
21) Atom numberings of the adducts are shown in Chart 3 and Fig. 7.

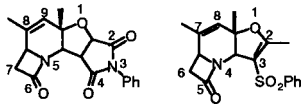

Fig. 7

22) Georg G. I., He P., Kant J., Wu Z., *J. Org. Chem.*, **58**, 5771—5778 (1993).
23) Taylor E. C., Mckillop A., Hawks G. H., *Org. Synth.*, **52**, 36—38 (1972).
24) *teXsan*: Crystal Structure Analysis Package, Version 1.11. Molecular Structure Corporation, Rigaku Corporation, 2000.